Desalination and Water Treatment
www.deswater.com
doi: 10.5004/dwt.2023.29656

298 (2023) 81–92
June

Treatment of water contaminated by cadmium using low-cost and eco-friendly alginate/Moroccan clay composite beads

Younes Rachdi[a,*], Marouane El Alouani[b], Rajaa Bassam[a], El Hassane Mourid[c], Hamid Saufi[b], El Hassan El Khattabi[d], Fadoua El Makhoukhi[e], El Hassane Khouya[a], Said Belaaouad[a]

[a]*Laboratory of Physical Chemistry of Materials LCPM, Faculty of Sciences Ben M'Sik, Hassan II University of Casablanca, B.P.7955, Bd Cdt Driss El Harti, Casablanca, Morocco, emails: rachdi.smc@gmail.com (Y. Rachdi), bassam.rajaa@gmail.com (R. Bassam), e.khouya@crmefsm.ac.ma (E.H. Khouya), belaaouad.s@gmail.com (S. Belaaouad)*
[b]*Laboratory of Physico-Chemistry of Inorganic and Organic Materials (LPCIOM), Materials Science Centre (MSC), Mohammed V University, Ecole Normale Superieure (ENS), Rabat, Morocco, emails: ma.elalouani@gmail.com (M. El Alouani), saufihamid@yahoo.fr (H. Saufi)*
[c]*Department of Chemistry, Physical Chemistry of Materials Team, High Training Teachers School, Cadi Ayyad University, Marrakech, Morocco, email: mourice.smc@gmail.com (E.H. Mourid)*
[d]*Laboratory of Sciences and Process Optimization (SCIMATOP), Faculty of Sciences Semlalia, Cadi Ayyad University Marrakech, Morocco, email: eelkhattabi36@gmail.com (E.H. El Khattabi)*
[e]*The National Center for Scientific and Technical Research, Mohammed V University, Rabat, Morocco, email: fadoua10@gmail.com (F. El Makhoukhi)*

Received 18 December 2022; Accepted 29 May 2023

ABSTRACT

This study aims to investigate the batch mode adsorption of Cd(II) from an aqueous solution using two adsorbents: raw clay without any treatment (NC) and clay composite beads (CCB). The adsorbents before and after adsorption were characterized using several techniques such as X-ray fluorescence, X-ray diffraction, Fourier-transform infrared, scanning electron microscopy, energy-dispersive X-ray, thermogravimetric analysis, differential thermal analysis and zeta potential. The influence of the experimental parameters of adsorption such as mass, pH, concentration, contact time, and temperature were studied to optimize them. The results of the kinetic study suggest that the adsorption of Cd(II) by NC and CCB can be explained by the pseudo-second-order kinetic model. The time after which the adsorption reaction does not evolve was 120 min for both adsorbents. The Langmuir isotherm model was found to be the most adequate for Cd(II) adsorption, with maximum adsorption capacities of 42.97 and 100.8 $mg \cdot g^{-1}$ for NC and CCB, respectively. The thermodynamic parameters indicated that the adsorption mechanism of Cd(II) on the surface of NC and CCB was endothermic, spontaneous, and favorable with a random distribution of Cd(II) ions at the solid/liquid interface. The regeneration study showed that NC and CCB are recyclable with. These findings suggest that NC and CCB could be used as effective and environmentally friendly adsorbents for treating heavy metal contamination in effluents.

Keywords: Adsorption; Natural clay; Clay composite beads (CCB); Regeneration; Cadmium Cd(II)

* Corresponding author.

1944-3994/1944-3986 © 2023 Desalination Publications. All rights reserved.

1. Introduction

In the last years, the World Environmental Protection Organization has been ringing the alarm bell about aquatic pollution by heavy metals coming from human activities. Wastewater charged with heavy metals comes from several sources. The surface treatment and electroplating industry generates the largest amount of effluent contaminated with heavy metals [1]. Other industries are also responsible for the contamination of wastewater by heavy metals such as paper, batteries, pesticides, textile dyeing, paint, and others [2]. The toxicity, non-biodegradability, and bioaccumulation of these pollutants are major problems for human health and the ecosystem [3]. Cadmium is among the heavy metals that have a harmful effect on the environment and living beings. it's known by their human carcinogen character [1]. The maximum concentration of cadmium in drinking water should not exceed 0.03 $mg \cdot L^{-1}$ according to the World Health Organization (WHO) [4]. As a result of these dangerous effects on human health, the environment, and the ecosystem, several treatment processes are developed to remove these pollutants, such as chemical precipitation, flocculation, ion-exchange, electrolysis, membrane processes, and adsorption [5]. Among these processes, adsorption is an efficient and inexpensive method for the treatment of water contaminated by organic and inorganic pollutants. Several studies are focused on the use of low-cost materials for the treatment of aqueous solutions contaminated by cadmium, such as, such adsorbing power of clays as activated carbon [6], chitosan [7], modified kaolin [8], zeolite [9], biomass [10], and other adsorbents. Activated carbon has been among the most used classical adsorbents for the removal of water contaminated with Cd(II), but its expensive cost is a great disadvantage, hence the search for new materials that are less expensive and have higher removal capacity, such as clays and their by-products.

Morocco is known by its vast clay deposits. Clays are constituted by minerals whose particles are essentially phyllosilicates [11]. This type of structure leads to an interesting texture associated with very particular physico-chemical characteristics [12], which explains the adsorption capacity of clays. Several studies have proven that clays are effective adsorbents for the treatment of wastewater loaded with heavy metals. For examples: treatment of aqueous solutions contaminated by Cd(II) using Moroccan natural clays [3], bentonite [13], Turkish illitic clay [14], and natural clay southern Tunisian [15]. Many studies have also shown the low adsorption capacity of Cd(II) by clay [16–18], but it could be increased by thermal and chemical treatment, purification or modification [19]. The improvement of the adsorption capacity of clays using sodium alginate-clay composites is a current topic. Alginates are non-toxic and biodegradable polymers, and their use in the clay modification process allows the production of low-cost composites with improved adsorption properties [19].

In this context, the objective of this work is to synthesize a new adsorbent based on Moroccan clays and alginates to elaborate alginate-clay composite beads. Then to study the adsorption efficiencies of Cd(II) in aqueous solution by the raw clays and the synthesized beads. The influence of experimental adsorption parameters such as adsorbent mass, contact time, pH, temperature, and initial pollutant concentrations was studied to determine the optimal adsorption conditions. The isotherms, thermodynamics, and kinetics of adsorption were studied to understand the interaction of Cd(II) in its ionic form with the used adsorbents. The regeneration of the adsorbents after adsorption was also studied to evaluate their efficiency.

2. Materials and methods

2.1. Materials and chemicals

The clay used as adsorbent was collected in the region of Sidi Moussa El Mejdoub located 12 km north of the city of Casablanca in central Morocco. The adsorbent was crushed and then sieved to obtain particles with a diameter lower than 200 μm. The pollutant used as adsorbate is Cd(II) marketed as $CdCl_2$ distributed by Labo Chimie with a purity higher than 99%. Sodium alginate, sodium hydroxide (NaOH, 99%), and calcium chloride ($CaCl_2$, 99%), used for the preparation of the clay beads were provided by Sigma-Aldrich (Germany).

2.2. Preparation of beads

The protocol for preparing the clay composite beads (CCB) is as follows: First, 2 g of sodium alginate ($C_6H_7O_6Na$) powder is added to 100 mL of distilled water and stirred for 2 h until the solution becomes homogeneous. Next, 2 g of natural clay (NC) is added slowly to the suspension and stirred rapidly for 2 h to obtain a well-homogeneous gel. To form the beads, a syringe pump is used to prepare perfectly spherical drops, which fall into 200 mL of a 1M calcium chloride solution ($CaCl_2$) under magnetic stirring. The mixture is then left to cure for 24 h in a cold environment. After maturation, the beads are filtered and washed several times with distilled water to remove any excess calcium chloride.

2.3. Adsorbents characterization

The Axios X-ray Fluorescence spectrometer was used to determine the composition of NC. The crystalline phases of NC and CCB were identified using Bruker Binary V4 X-ray diffractometer. The FTIR spectrometer Bruker Tensor 27 (Germany) was used to determine the functional groups of NC and CCB before and after adsorption. The JEOL 6300 (Japan) scanning electron microscope (SEM) coupled with energy-dispersive X-ray (EDX) were used to study the microstructure and composition of the adsorbents before and after adsorption. The Malvern zetameter (United Kingdom) was used to measure the zeta potential of adsorbents at different acid pH. The cation exchange capacity (CEC) was determined by the hexamine-cobalt method. Thermogravimetric analysis (TGA) and differential thermal analysis (DTA) analysis was carried out using LabsysTM Evo (1F) Setaram Instrument (France), operating in a temperature range between 20°C and 800°C under air flow of 45 $mL \cdot min^{-1}$. The concentration of Cd(II) was determined using Inductively Coupled Plasma Mass Spectrometry (ICP-MS) by the PerkinElmer model (Germany).

2.4. Batch adsorption studies

Adsorption experiments were performed with constant stirring (250 rpm) to optimize experimental parameters such as adsorbents doses (0.025–0.5 g/L), initial solution pH (1–6), contact time (0–220 min), initial adsorbate concentration (20 to 200 mg·L^{-1}), and temperature (25°C–45°C). The pH of the solution was adjusted using NaOH (0.1 M) and HCl (0.1 M) solutions. After adsorption, the obtained mixtures were centrifuged at 4,000 rpm for 10 min, in order to determine the residual concentration. The amounts of Cd(II) retained by the materials were determined using the following equation.

$$Q = \frac{(C_0 - C)V}{m} \quad (1)$$

where Q (mg·g^{-1}) is the amount of pollutant adsorbed per unit mass of the adsorbents, C and C_0 (mg·L^{-1}) are respectively the concentration of Cd(II) after and before adsorption, V (L) is the volume of the solution, and m (g) is the mass of materials used in the test.

2.5. Regeneration study

The recycling of NC and CCB contaminated by Cd(II) after adsorption was performed by washing with a concentrated hydrochloric acid solution (1 M). The washing time and the agitation speed were respectively 1h and 450 rpm, After the desorption process, the concentration of Cd(II) can be determined by the ICP-MS technique to evaluate the effectiveness of the recycling process.

3. Results and discussion

3.1. Characterization of NC and CCB

3.1.1. X-ray fluorescence analysis

Table 1 shows the results of the analysis of the chemical composition analysis of NC by X-ray fluorescence. The obtained results indicate that the following oxides constitute 95.21% of the total mass of NC: Fe_2O_3, Al_2O_3, MgO, and CaO. Although NC also contains K_2O and Na_2O, their content does not exceed 4.79%. The chemical composition of NC, rich in oxides, leads to a high concentration of exchangeable ions such as Fe^{2+}, Mg^{2+}, Al^{3+}, and K^+, which favor the adsorption of heavy metals [20].

3.1.2. X-ray diffraction analysis

The diffractograms of NC and CCB obtained by X-ray diffraction are illustrated in Fig. 2. The analysis of the obtained diagrams shows characteristic peaks of palygorskite at 25.3°, 27.48°, and 29.78°. The peaks appear at 17.78°, 19.76°, 26. 64°, 27.94°, 34.72°, 37.8°, 45.38° and 61.64° indicate the presence of muscovite, while peaks at 31.82°, 41.08°, 44.72°, 50.06° and 67.68° correspond to reflections of ankerite. The presence of kaolinite was confirmed by their characteristic reflections located at 12.46°, 23.42°, and 31.82°. Quartz is also present with reflections at 20.96°, 26.64°, 36.54°, 39.44°, 40.28°, 42.4°, 50.16°, 50.92°, 59.96°, 67.68°, 68.16° and 68.54°. The pic located at 30.08° corresponds to the reflection of dolomite. The preparation of CCB did not result in a change in the location of the peaks due to the incapacity of the alginate to intercalate between the layers of clay minerals [21,22].

Table 1
Mineral composition of natural clay

Component (%)	Natural clay
Na_2O	0.287
Al_2O_3	18.981
SiO_2	53.317
Fe_2O_3	3.478
K_2O	1.361
MgO	8.581
CaO	10.843
Other	3,152

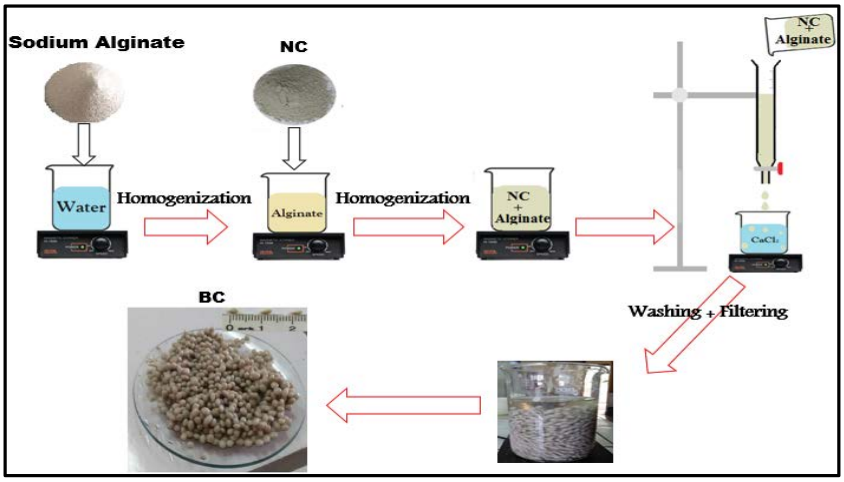

Fig. 1. Schematic presentation of the clay composite beads preparation protocol.

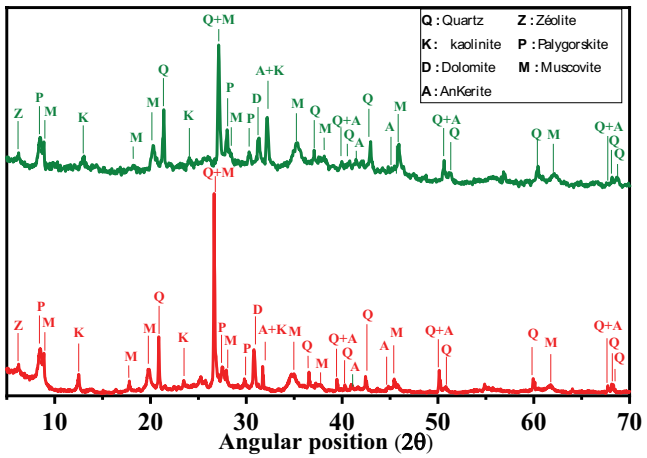

Fig. 2. X-ray diffraction patterns of natural clay and clay composite beads.

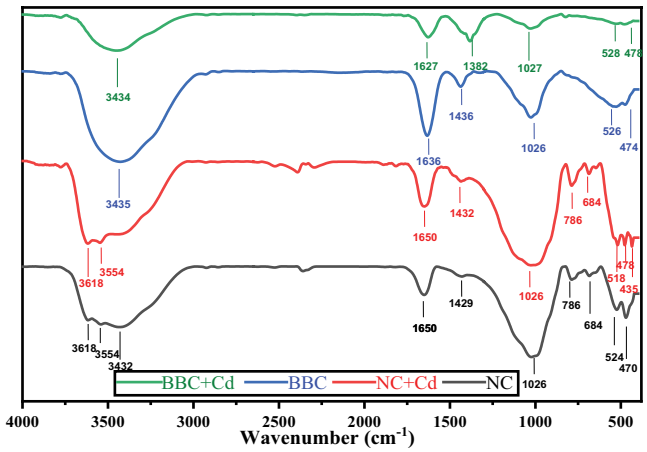

Fig. 3. Fourier-transform infrared spectra before and after adsorption of natural clay and clay composite beads.

3.1.3. Fourier-transform infrared analysis

The Fourier-transform infrared (FTIR) spectra of NC and CCB after and before Cd(II) adsorption are shown in Fig. 3. The spectrum analysis of NC shows the presence of the bands at 470, 524, and 786 cm^{-1} related to Si–O–Si, Si–O–Al, and Al–OH deformation, respectively [23]. The Si–O stretching vibration was confirmed by the bands located at 684 and 1,026 cm^{-1} [24,25]. The bands located at 1,650; 3,552 and 3,432 cm^{-1} related to the –OH stretching vibration of the coordinated and zeolitic water molecule [26]. The band appearing around 1,430 cm^{-1} can be due to the O–C–O bonding vibration of dolomite [27]. The band located at 3,618 cm^{-1} corresponds to the –OH stretching vibration of M–OH (M: Mg, Al, Fe) [26]. For the CCB spectrum, an intense band was observed at 3,435 cm^{-1} due to the vibration of the hydroxyl groups present in the alginate structure. In addition, the band at 1,650 cm^{-1} was intercalated towards the low-frequency 1,635 cm^{-1}, and an increase in their intensity due to the overlap made by the carbonyl group (–COO) of alginate [28]. After adsorption, the FTIR spectrum is almost identical with a change in intensity due to the participation of all the functional groups on the surface of NC and CCB in the adsorption process [20]. For NC a band appeared at 435 cm^{-1} due to the Cd–O vibration which confirms the fixation of Cd(II) by the surface of NC [4].

3.1.4. SEM analysis

SEM images of NC and CCB before and after Cd(II) adsorption are illustrated in Fig. 4. The analysis of the images obtained for NC and CCB before adsorption showed a heterogeneous and porous surface containing particles as aggregates that formed cavities. A fibrous structure was observed in the sample of NC due to the presence of palygorskite. It is clearly visible that the morphology of CCB was rich in pores compared to NC. After adsorption, the surface of both adsorbents becomes homogenous due to the formation of a smooth layer on the surface resulting from the Cd(II) adsorption. The number of pores tended to decrease significantly due to their saturation by Cd(II) ions.

3.1.5. EDX analysis

The EDX analysis of NC and CCB before and after adsorption are presented in Fig. 5. The comparison of the spectra showed a higher percentage of element O in the structure of CCB compared to NC due to the presence of alginate in its structure. Additionally, the presence of Ca peaks and the increase in the percentage of Cl can be explained by the use of $CaCl_2$ solution during the synthesis of CCB. After the adsorption, the appearance of Cd(II) peaks on the spectra shows that the Cd(II) ion was successfully adsorbed on the surface of both adsorbents.

3.2. Thermogravimetry analysis

The results of TGA and DTA of NC are presented in Fig. 6. The first weight loss observed in the temperature range of 50°C–230°C was attributed to the evaporation of adsorbed water and corresponded to the first DTA peak observed at 80°C. The second weight loss observed between 200°C and 400°C was attributed to the combustion of residual organic matter. The third weight loss observed between 400°C and 600°C was attributed to the dehydroxylation of kaolinite present in NC and the consequent formation of metakaolinite, which was supported by the DTA peak observed at 513°C. Above 600°C, the mass of the sample continued to decrease due to the removal of residual hydroxyl groups from muscovite.

3.3. Physico-chemical properties

In this study, two physicochemical properties were determined for the samples: zeta potential and CEC. The zeta potential was used to determine the surface charge of the materials. The variation of the zeta potential of CCB and NC with pH is presented in Fig. 7. This result indicates that both materials possess a negative surface charge across all pH ranges studied and the zeta potential decreases with increasing pH. A high CEC value of 85 meq/100 g was observed for NC, indicating its high ion exchange capacity and swelling character.

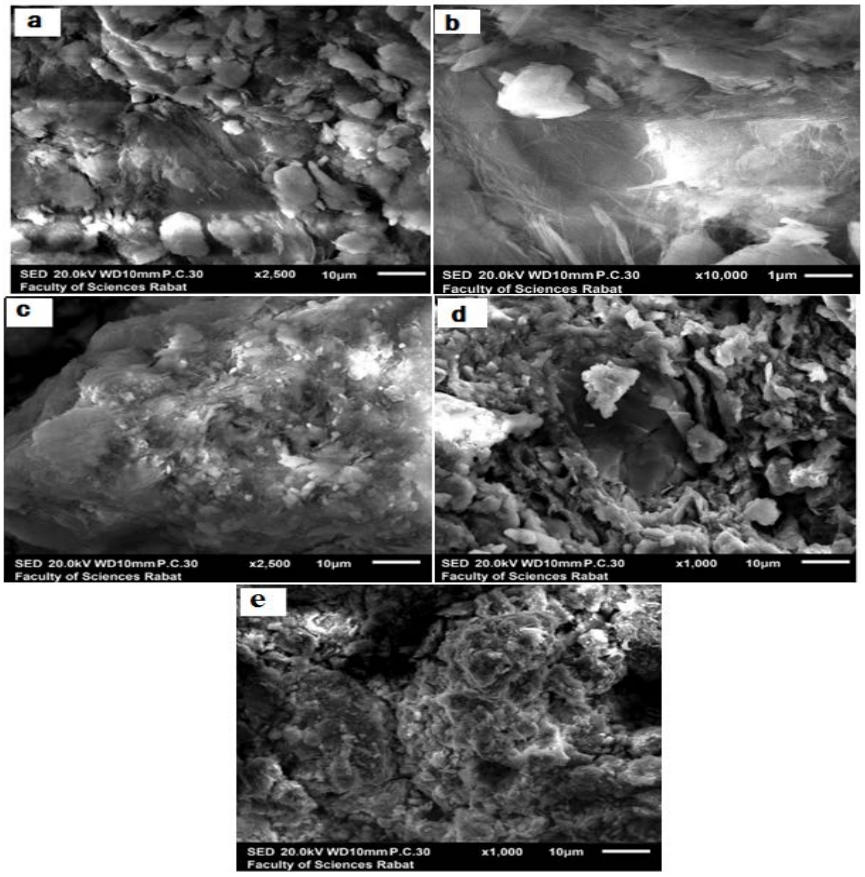

Fig. 4. Scanning electron microscopy images of natural clay (a,b), NC + Cd(II) (c), clay composite beads (d), and CCB + Cd(II) (e).

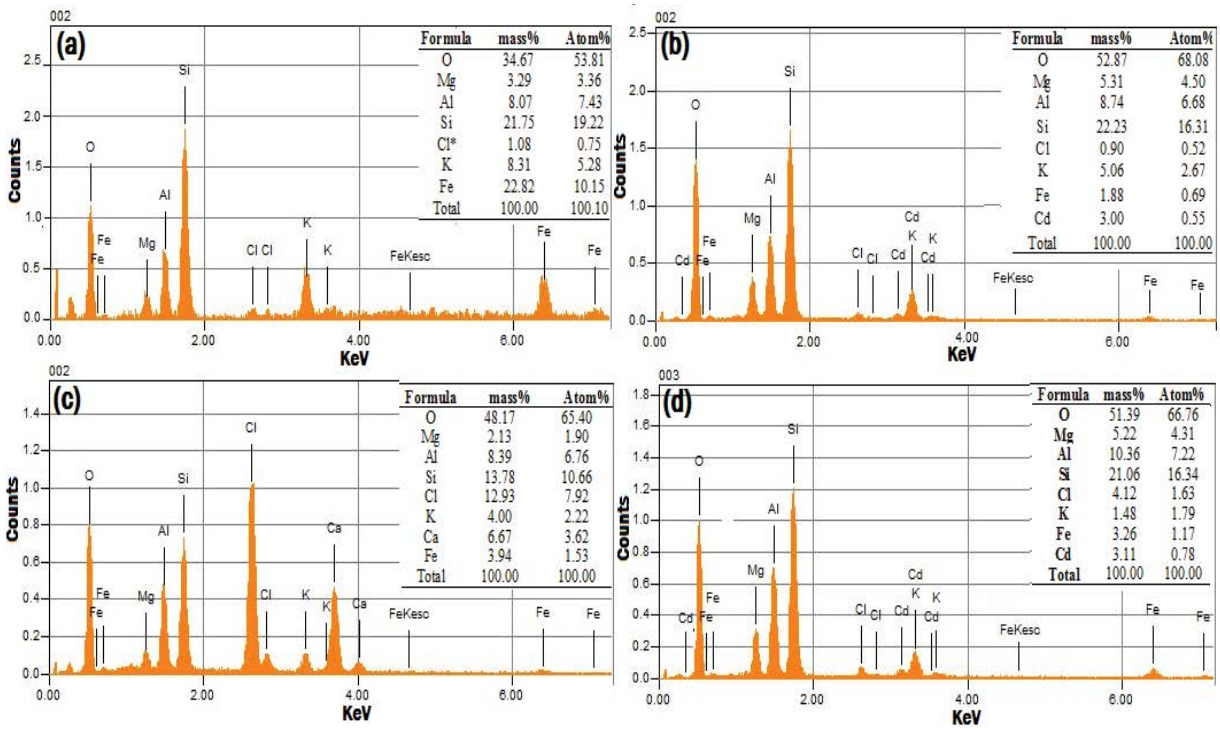

Fig. 5. Energy-dispersive X-ray spectroscopy patterns of natural clay (a), NC + Cd(II) b), clay composite beads (c), and CCB + Cd(II) (d).

3.4. Adsorption study

3.4.1. Effect of adsorbent dosage

The effect of NC and CCB mass on Cd(II) retention is a very important parameter to determine the optimal mass used in the adsorption processes. The influence of the adsorbent mass was studied for masses ranging from 0.25 to 10 g·L^{-1}, initial concentration 100 mg·L^{-1}, pH of the solution, contact time of 120 min, room temperature, and constant stirring speed of 450 rpm. The results obtained in Fig. 8 show an increase in the percentage of Cd(II) elimination with an increase of adsorbent mass, which can be explained by an increase in the active adsorption sites [13]. However, the quantity of Cd(II) adsorbed per unit mass decreases with the increase of the mass of NC and CCB due to the problem of access of Cd(II) ions to the active adsorption sites caused by the aggregation of the adsorbent particles [24]. Beyond 2 g·L^{-1} for NC and 1 g·L^{-1} for CCB, the adsorption percentage becomes constant due to the decrease of the driving force for mass transfer at a low concentration of Cd(II) in the solution [25]. The optimal masses of NC and CCB are respectively 2 and 1 g·L^{-1}.

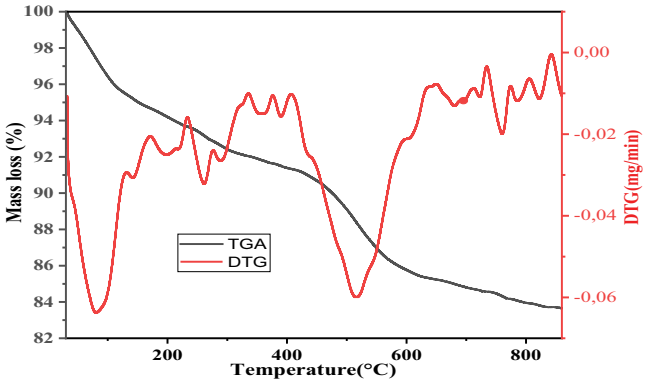

Fig. 6. Thermogravimetric analysis and differential thermal analysis diagrams of natural clay.

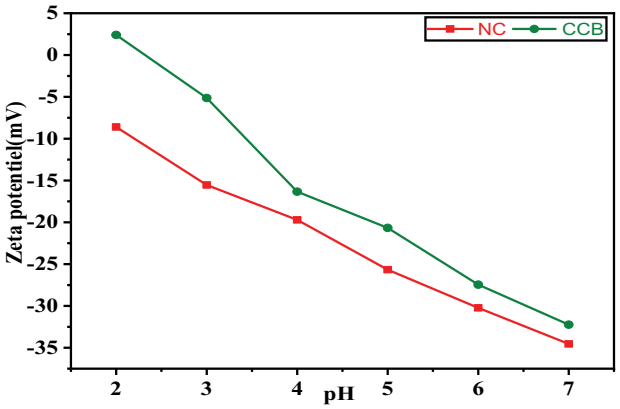

Fig. 7. Variation of the zeta potential of clay composite beads and natural clay according to the pH.

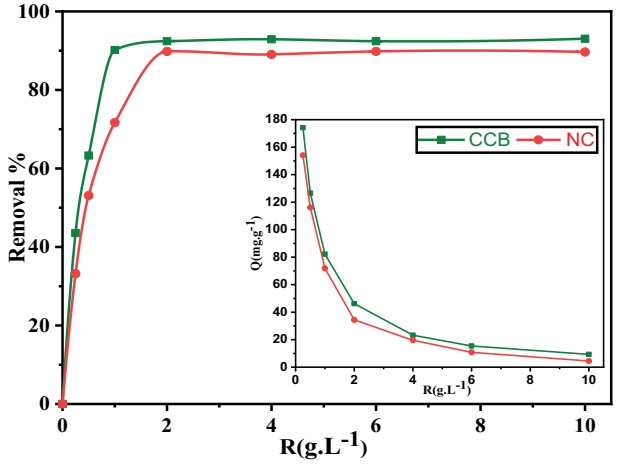

Fig. 8. Effect of natural clay and clay composite beads dosage on the adsorption of Cd(II).

3.4.2. Effect of initial pH

The effect of initial pH was studied for pH values ranging from 2 to 6, initial concentration 100 mg·L^{-1}, adsorbents masses, respectively 2 and 1 g·L^{-1} for NC and CCB, contact time 120 min, room temperature, and constant stirring speed 450 rpm. The effect of basic pH was not studied due to the precipitation of Cd(II) in the form of hydroxide $Cd(OH)_2$ [4]. The results obtained in Fig. 9 show a significant increase in the adsorption capacities of the adsorbents as the pH increases. This can be attributed to the deprotonation of the hydroxide groups on the basal surface of the clay minerals, specifically the silanol and aluminol groups, as the pH increases. This creates negative sites that facilitate the attraction of Cd(II). Conversely, at lower acidic pH values, it was observed that the adsorption capacity of dyes decreased, as the presence of H^+ ions in the medium competed with Cd(II) for the available site. This result suggests that the adsorption process can be defined by a electrostatic mechanism.

3.4.3. Effect of contact time

The effect of contact time was studied for values ranging from 1 to 240 min, an initial cadmium concentration

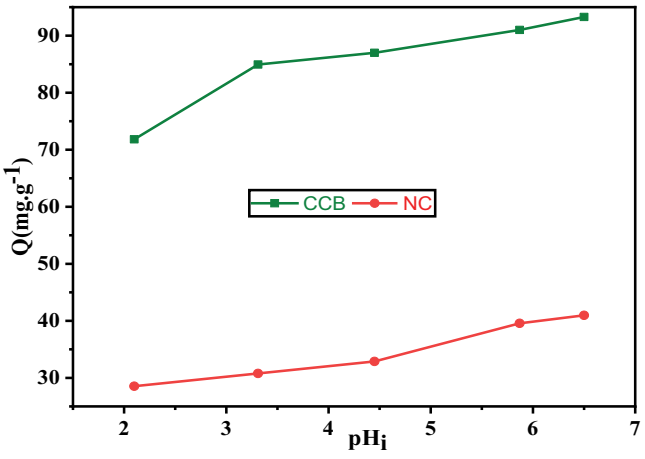

Fig. 9. Effect of initial pH on the adsorption of Cd(II) by natural clay and clay composite beads.

100 mg·L^{-1}, adsorbent masses of 1 and 2 g·L^{-1} for NC and CCB, respectively, initial solution pH, room temperature, and a constant stirring speed of 450 rpm. The results obtained in Fig. 10 indicate that during the first 30 min of the adsorption experiment, there was a rapid increase in the quantity of Cd(II) ions adsorbed by NC and CCB, then becomes slow with time until equilibrium. This result can be explained by the availability of active adsorption sites at the beginning of the experiment. Over time, the number of available sites decreased until total saturation [26]. The equilibrium times are 120 min for NC and CCB.

3.4.4. Effect of initial concentration

The effect of initial concentration was studied for values ranging from 20 to 200 mg·L^{-1}, adsorbent masses of 2 and 1 g·L^{-1} for NC and CCB, respectively, initial solution pH, contact time 120 min, room temperature, and a constant stirring speed of 450 rpm. The results obtained in Fig. 11 show that the efficiency of the adsorption process was high when the initial concentration of the pollutants is low. It attains a percentage of elimination close to 98% for the two adsorbents when the initial concentration 20 mg·L^{-1}. This result can be attributed to the existence of a sufficient number of active adsorption sites [20]. An increase in the initial concentration of the solution leads to a significant increase in the quantity of cadmium ions adsorbed. This is attributed to the enhanced diffusion of the ions Cd(II) from the solution towards the surface of the adsorbents [13]. After 100 mg·L^{-1} for NC and 120 mg·L^{-1} for CCB the adsorbents do not continue to adsorb because most of the active adsorption sites are occupied by cadmium (saturation) [4].

3.4.5. Effect of temperature

The effect of temperature on the adsorption of cadmium by NC and CCB was studied for temperatures ranging from 25°C to 45°C, adsorbent masses of 2 and 1 g·L^{-1} for NC and CCB, respectively, pH of the initial solution, contact time of 120 min, initial concentration 100 mg·L^{-1} and a constant stirring speed of 450 rpm. The results obtained in Fig. 12 show an increase in the adsorption capacity with the increase in temperature due to the endothermic character of the adsorption reaction between cadmium and the surface of NC and CCB [27].

3.5. Kinetic study

Pseudo-first-order, pseudo-second-order, and intraparticle diffusion kinetic models were used to describe the adsorption kinetics and determine their limit step [29]. The linear equations of the kinetic models and their parameters are illustrated in Table 2.

The plot of the linear form of these models is illustrated in Fig. 12a and b. The kinetic parameters such as kinetic constants and correlation coefficients are shown in Table 3. It is clearly from the table that the correlation coefficient values R^2 of the pseudo-second-order model are higher than

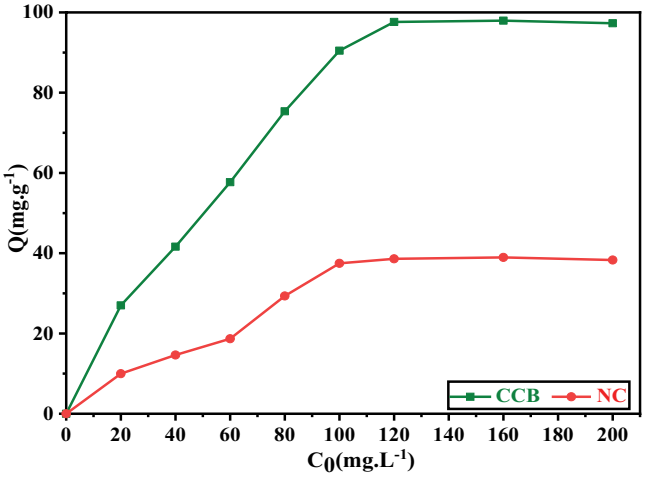

Fig. 11. Effect of initial concentration on the adsorption of Cd(II) by natural clay and clay composite beads.

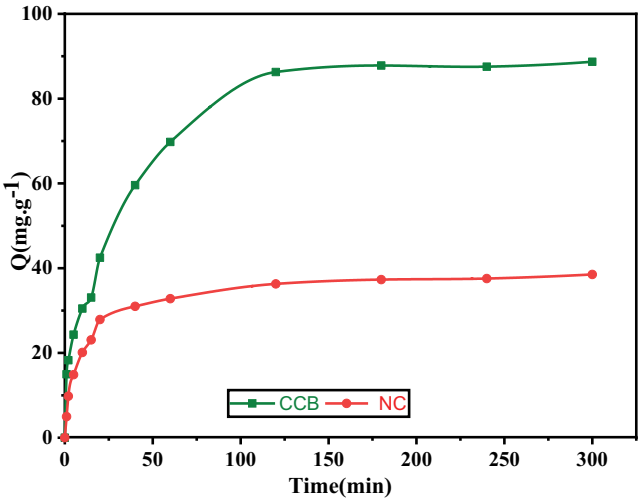

Fig. 10. Effect of contact time on the adsorption of Cd(II) by natural clay and clay composite beads.

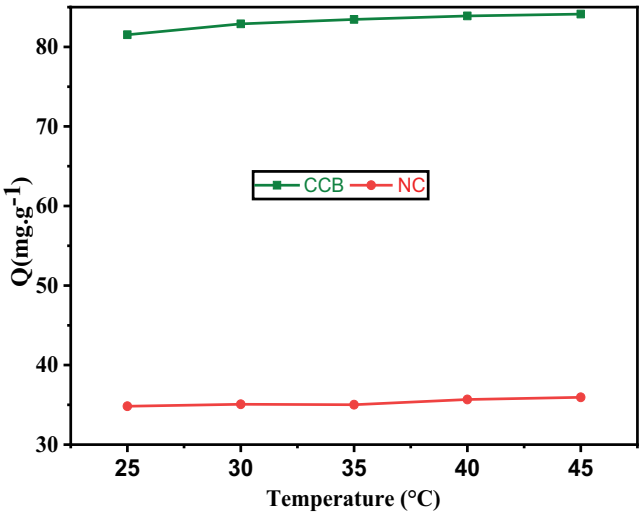

Fig. 12. Effect of temperature on the adsorption of Cd(II) by natural clay and clay composite beads.

Table 2
Linear equations of the kinetic models and their parameters

	Model	Linear equation	Parameters
Kinetic model	Pseudo-first-order	$\ln(Q_e - Q_t) = \ln(Q_e) - K_1 t$	Q_t: is the quantity retained by the adsorbent at time t (mg·g^{-1}) Q_e: the quantity retained by the adsorbent at equilibrium (mg·g^{-1}) K_1: is the pseudo-first-order rate constant (min^{-1}) K_2: is the pseudo-second-order rate constant (g·mg^{-1}·min^{-1}) K_3: is the rate constant of intraparticle diffusion (mg·g^{-1}·min$^{-0.5}$) C: is a constant (mg·g^{-1})
	Pseudo-second-order	$\frac{t}{Q_t} = \frac{1}{Q_e} t + \frac{1}{K_2 Q_e^2}$	
	Intraparticle diffusion	$Q_t = K_3 t^{0.5} + C$	

Table 3
Kinetic parameters for the adsorption of Cd(II) by natural clay and clay composite beads

Adsorbents	Q_{exp} (mg·g^{-1})	Pseudo-first-order			Pseudo-second-order			Intraparticle diffusion		
		K_1 (min^{-1})	R^2	Q_e (mg·g^{-1})	K_2 (g·mg^{-1}·min^{-1})	Q_e (mg·g^{-1})	R^2	K_{in1}	K_{in2}	K_{in3}
Natural clay	37.29	0.014	0.91	6.14	0.003	38.75	0.992	6.74	16.08	0.31
Clay composite beads	88.70	0.0088	0.93	20.03	0.0006	94.69	0.999	7.04	9.27	0.33

that of the pseudo-first-order for both adsorbents and the experimentally adsorbed quantities are adjacent to those calculated from the pseudo-second-order model. Therefore, the pseudo-second-order model can explain the retention of cadmium by NC and CCB. This result indicates that the interaction between Cd(II) and the surface of NC and CCB is chemical in nature (chemisorption) [20].

The diffusion mechanism was studied using the intraparticle diffusion model. The multilinear plot obtained in Fig. 13c indicates that the adsorption process of Cd(II) by NC and CCB occurs in three steps. The first step: the migration of cadmium ions from the aqueous solution to the external surface of NC and CCB, the second step: the intraparticle transfer of Cd(II) ions, and the third step: the fixation of ions on the surface of adsorbents [30]. The correlation coefficient R^2 of the first stage are the highest which indicates that the rate of adsorption was controlled by the transfer of cadmium ions to the external surface of the adsorbent.

3.6. Adsorption isotherm

The Freundlich and Langmuir models were used to analyze the experimental data and study the distribution of Cd(II) between the solid and liquid phases [20]. The linear equations of the isotherm models and their parameters are presented in Table 4.

The plot of the linear form of the Langmuir and Freundlich isotherms is shown in Fig. 14 and their corresponding parameters are summarized in Table 5. The comparison of the correlation coefficients of the Langmuir and Freundlich isotherms allows us to conclude that the isotherm explaining the adsorption of cadmium by NC and CCB is the Langmuir isotherm because of their highest correlation. This result indicates monolayer adsorption occurs between the Cd^{2+} ions on the homogeneous surface of both adsorbents [20]. The values of the separation factor R_L were 0.99 and 0.98, respectively for CCB and NC which indicates that the adsorption of Cd(II) on both adsorbents is favorable because $0 < R_L < 1$ [20]. The Langmuir constant (K_L) for Cd(II) adsorption on CCB is higher than that of adsorption on NC which indicates that the interaction between Cd(II) and the active adsorption sites is stronger with CCB compared to NC [24]. The maximum adsorption capacities obtained are 42.97 and 100.8 mg·g^{-1}, respectively for NC and CCB.

3.7. Thermodynamic study

The thermodynamic parameters such as Gibb's free energy $\Delta G°$, enthalpy $\Delta H°$ and entropy ΔS allow to understand the effect of temperature and to determine the nature of the adsorption reaction [31]. The thermodynamic equations and their parameters are presented in Table 6.

The thermodynamic parameters presented in Table 7 indicate negative values of $\Delta G°$, which suggest that the adsorption reaction of Cd(II) ions on NC and CCB was spontaneous and thermodynamically favorable. The positive value of $\Delta H°$ confirmed the endothermic nature of the adsorption reaction between Cd(II) and the surface of NC and CCB. The positive values of $\Delta S°$ indicated a random distribution of Cd(II) at the adsorbent/liquid interface during the adsorption process. These findings were consistent with previous studies in the literature on the adsorption of cadmium [5,32].

3.8. Regeneration of NC and CCB

The regeneration of materials is one of the methods used to confront the decrease in natural resources and their high prices. Several regeneration methods were developed by researchers including, such as microwave regeneration, chemical regeneration, oxidation regeneration, thermal regeneration, and other techniques. In this study, the regeneration of NC and CCB was carried out by the

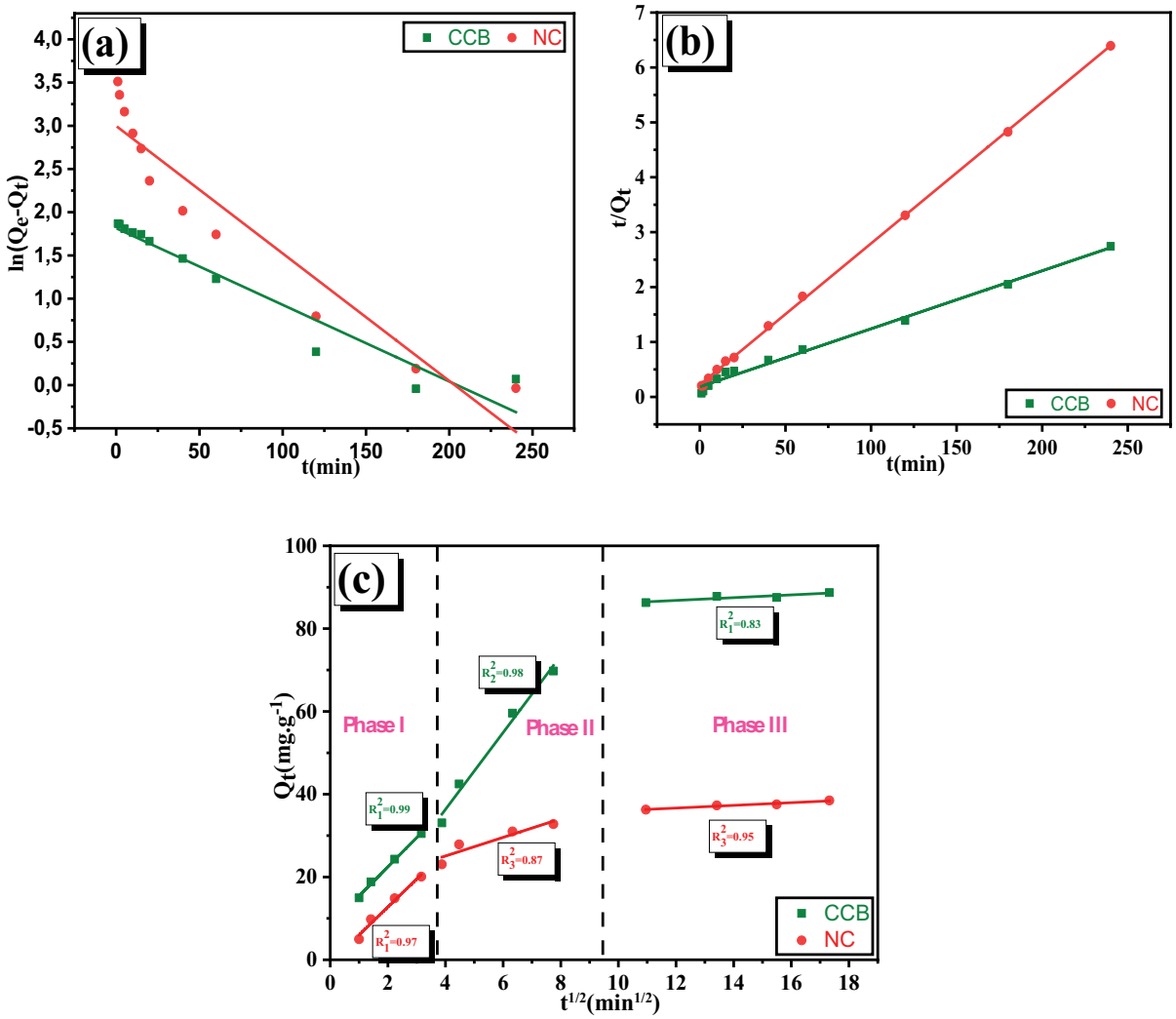

Fig. 13. Kinetic models for the adsorption of Cd(II) by natural clay and clay composite beads: (a) pseudo-first-order, (b) pseudo-second-order and (c) intraparticle diffusion.

Table 4
Linear equations of isotherms models and their parameters

	Model	Linear equation	Parameters
Isotherm model	Langmuir	$\ln Q_e = \frac{1}{n} C_e = \ln K_F$	Q_e: the quantity retained by the adsorbent at equilibrium (mg·g^{-1}) Q_{max}: is the maximum quantity of pollutant retained by the adsorbent (mg·g^{-1}) C_e: is the concentration of Cd(II) at equilibrium (mg·L^{-1}) K_L: is the Langmuir constant (L·mg^{-1}) K_F: is the Freundlich constant $1/n$: is the Freundlich constant which indicates the intensity of the adsorption
	Freundlich	$\ln Q_e = \frac{1}{n} C_e = \ln K_F$	

chemical method using a hydrochloric acid solution. The results, shown in Fig. 15, indicate that after four cycles of regeneration, the percentage of Cd(II) desorption reached 61.13% and 70.01% for NC and CCB, respectively. The significant efficiency of the change over the cycles demonstrates the regeneration capacity of NC and CCB.

3.9. Comparative study

Table 8 compares the maximum adsorption capacity of NC and CCB for cadmium removal with other adsorbents. It is clear that the adsorption capacity of CCB and NC is higher than some other materials listed in the literature. This difference may be due to variations in the

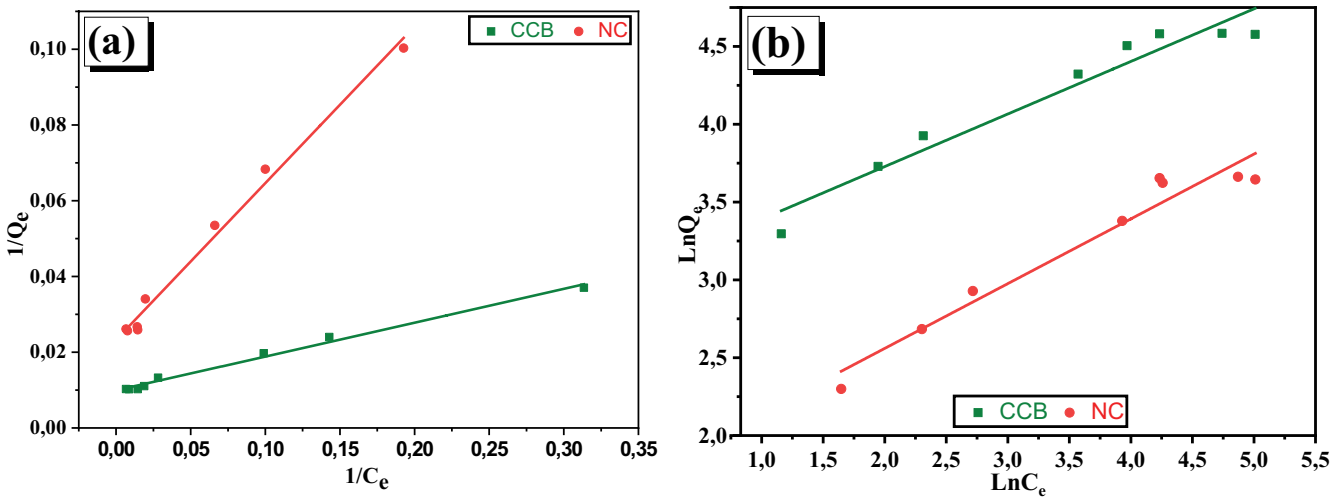

Fig. 14. Adsorption isotherms of Cd(II) onto natural clay and clay composite beads. (a) Freundlich and (b) Langmuir isotherm models.

Table 5
Freundlich and Langmuir isotherms model constants

	Langmuir constants				Freundlich constants		
	Q_{max} (mg·g^{-1})	K_L (L·g^{-1})	R^2	R_L	K_F (mg·g^{-1})	$1/n$	R^2
Natural clay	42.97	0.056	0.994	0.99	5.58	0.42	0.95
Clay composite beads	100.8	0.11	0.998	0.98	21.1	0.33	0.94

Table 6
Thermodynamic equations and their parameters

Equations	Parameters
$\Delta G° = -RT \ln K_D$	R: is the universal perfect gas constant (R = 8.314 J·mol^{-1}·K^{-1})
$K_D = \frac{Q_e}{C_e}$	T: is the absolute solution temperature
	K_D: is the distribution coefficient
$\ln K_D = \frac{\Delta S°}{R} - \frac{\Delta H°}{RT}$	$\Delta G°$: free energy (J·mol^{-1}·K^{-1})
	$\Delta H°$: enthalpy (kJ·mol^{-1})
	ΔS: entropy (J·mol^{-1}·K^{-1})

Table 7
Thermodynamic parameters for the adsorption of Cd(II) using natural clay and clay composite beads

Adsorbents	$\Delta G°$ (kJ·mol^{-1})					$\Delta S°$ (kJ·mol^{-1}·K^{-1})	$\Delta H°$ (kJ·mol^{-1})
	Temperature (K)						
	298	303	308	313	318		
Natural clay	–11.785	–13.3	–15.423	–16.229	–18.599	0.183	45.184
Clay composite beads	–9.286	–10.706	–11.265	–11.958	–13.241	0.33	86.856

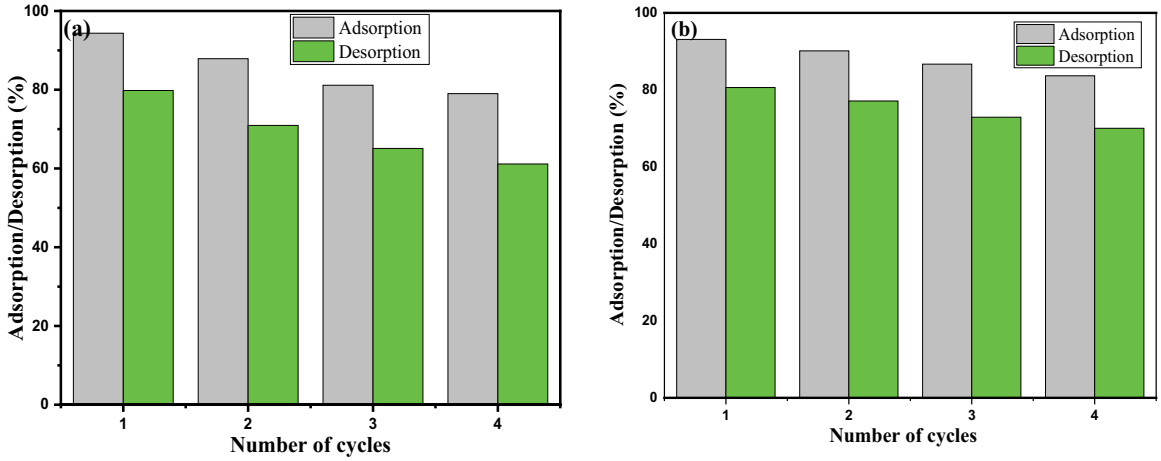

Fig. 15. Regeneration of natural clay (a) and clay composite beads (b).

Table 8
Comparison of the Cd(II) adsorption using different adsorbents

Adsorbents	Q_{max} (mg·g^{-1})	References
Modified Tanzanian Malangali kaolin clay	1.067	[5]
Clay of Tangier-Tétouan-Al Hoceima, Morocco	0.39	[16]
Moroccan clay QC-MC	4.23	[4]
Calcined Nigerian bentonite	1.38	[17]
Natural Nigerian bentonite	4.08	[17]
Moroccan clay QC-MT	5.85	[4]
Pure smectite	3.87	[18]
Lewatit S100	3.46	[18]
Silty clay	5.48	[33]
Natural clay	42.97	This study
Clay composite beads	100.8	This study

physical–chemical properties of the adsorbents, such as the specific surface area, CEC, material texture, and other properties.

4. Conclusion

In summary, this study compared the efficiency of natural clay (NC) and clay composite beads (CCB) for the removal of cadmium ions from synthetic aqueous solutions using batch adsorption experiments. The optimal experimental conditions were determined by varying the adsorbent mass, pH, concentration, temperature, and contact time. The results showed that the adsorption efficiency was higher at a pH close to 6.5. The kinetics of the adsorption process were modeled using the pseudo-second-order model, while the Langmuir isotherm model was found to be the most appropriate for describing the adsorption of Cd(II), with maximum adsorption capacities of 42.97 and 100.8 mg·g^{-1} for NC and CCB, respectively. The thermodynamic parameters indicated that the adsorption reaction was spontaneous, endothermic, and favorable, with a random distribution of Cd(II) at the adsorbent/liquid interface. The regeneration of NC and CCB was carried out using hydrochloric acid, and the results showed that both materials could be effectively recycled. Overall, this study demonstrated that NC and CCB are effective, low-cost, and reusable adsorbents for the treatment of Cd(II)-contaminated effluents.

Conflicts of interest

The authors declare that they have no conflicts of interest.

References

[1] M.A. Barakat, New trends in removing heavy metals from industrial wastewater, Arabian J. Chem., 4 (2011) 361–377.
[2] A.A.H. Saeed, N.Y. Harun, M.M. Nasef, A. Al-Fakih, A.A.S. Ghaleb, H.K. Afolabi, Removal of cadmium from aqueous solution by optimized rice husk biochar using response surface methodology, Ain Shams Eng. J., 13 (2022) 101516, doi: 10.1016/j.asej.2021.06.002.
[3] R. Bassam, M. El Alouani, J. Maissara, Y. Rachdi, N. Jarmouni, E.H. El Khattabi, M.E.M. Chbihi, S. Belaaouad, Enhanced removal of cadmium ions using Moroccan natural clays: characterization, kinetic, isotherm, thermodynamic, and regeneration investigations, Mater. Today Proc., 62 (2022) 6273–6280.
[4] R. Bassam, A. El hallaoui, M. El Alouani, M. Jabrane, E.H. El Khattabi, M. Tridane, S. Belaaouad, Studies on the removal of cadmium toxic metal ions by natural clays from aqueous solution by adsorption process, J. Chem., 2021 (2021) 7873488, doi: 10.1155/2021/7873488.
[5] B.K. Aziz, D.M.S. Shwan, S. Kaufhold, Characterization of Tagaran natural clay and its efficiency for removal of cadmium(II) from Sulaymaniyah industrial zone sewage, Environ. Sci. Pollut. Res., 27 (2020) 38384–38396.
[6] M. Ullah, R. Nazir, M. Khan, W. Khan, M. Shah, S.G. Afridi, A. Zada, The effective removal of heavy metals from water by activated carbon adsorbents of *Albizia lebbeck* and *Melia azedarach* seed shells, Soil Water Res., 15 (2019) 30–37.
[7] U. Upadhyay, I. Sreedhar, S.A. Singh, C.M. Patel, K.L. Anitha, Recent advances in heavy metal removal by chitosan-based adsorbents, Carbohydr. Polym., 251 (2021) 117000, doi: 10.1016/j.carbpol.2020.117000.
[8] H. Du, Z. Zhong, B. Zhang, D. Zhao, X. Lai, N. Wang, J. Li, Comparative study on intercalation-exfoliation and thermal activation modified kaolin for heavy metals immobilization

during high-organic solid waste pyrolysis, Chemosphere, 280 (2021) 130714, doi: 10.1016/j.chemosphere.2021.130714.
[9] S. Zhang, T. Lv, Y. Mu, J. Zheng, C. Meng, High adsorption of Cd(II) by modification of synthetic zeolites Y, A and mordenite with thiourea, Chin. J. Chem. Eng., 28 (2020) 3117–3125.
[10] M.W. Yap, N.M. Mubarak, J.N. Sahu, E.C. Abdullah, Microwave induced synthesis of magnetic biochar from agricultural biomass for removal of lead and cadmium from wastewater, J. Ind. Eng. Chem., 45 (2017) 287–295.
[11] S. Li, B. Mu, X. Wang, A. Wang, Recent researches on natural pigments stabilized by clay minerals: a review, Dyes Pigm., 190 (2021) 109322, doi: 10.1016/j.dyepig.2021.109322.
[12] A. Es-said, H. Nafai, G. Lamzougui, A. Bouhaouss, R. Bchitou, Comparative adsorption studies of cadmium ions on phosphogypsum and natural clay, Sci. Afr., 13 (2021) e00960, doi: 10.1016/j.sciaf.2021.e00960.
[13] B. Anna, M. Kleopas, S. Constantine, F. Anestis, B. Maria, Adsorption of Cd(II), Cu(II), Ni(II) and Pb(II) onto natural bentonite: study in mono- and multi-metal systems, Environ. Earth Sci., 73 (2015) 5435–5444.
[14] D. Ozdes, C. Duran, H.B. Senturk, Adsorptive removal of Cd(II) and Pb(II) ions from aqueous solutions by using Turkish illitic clay, J. Environ. Manage., 92 (2011) 3082–3090.
[15] L. Khalfa, A. Sdiri, M. Bagane, M.L. Cervera, Multi-element modeling of heavy metals competitive removal from aqueous solution by raw and activated clay from the Aleg formation (Southern Tunisia), Int. J. Environ. Sci. Technol., 17 (2020) 2123–2140.
[16] H. Es-sahbany, M.L. El Hachimi, R. Hsissou, M. Belfaquir, K. Es-sahbany, S. Nkhili, M. Loutfi, M.S. Elyoubi, Adsorption of heavy metal (Cadmium) in synthetic wastewater by the natural clay as a potential adsorbent (Tangier-Tetouan-Al Hoceima – Morocco region), Mater. Today Proc., 45 (2021) 7299–7305.
[17] J.A. Alexander, M.A.A. Zaini, S. Abdulsalam, U. Aliyu El-Nafaty, U.O. Aroke, Isotherm studies of lead(II), manganese(II), and cadmium(II) adsorption by Nigerian bentonite clay in single and multimetal solutions, Part. Sci. Technol., 37 (2019) 403–413.
[18] K. Bedoui, I. Bekri-Abbes, E. Srasra, Removal of cadmium(II) from aqueous solution using pure smectite and Lewatite S 100: the effect of time and metal concentration, Desalination, 223 (2008) 269–273.
[19] A. Oussalah, A. Boukerroui, Alginate-bentonite beads for efficient adsorption of methylene blue dye, Euro-Mediterr. J. Environ. Integr., 5 (2020) 31, doi: 10.1007/s41207-020-00165-z.
[20] R. Bassam, M. El Alouani, J. Maissara, Y. Rachdi, E.H. El Khattabi, H. Saufi, M. El Mahi Chbihi, S. Belaaouad, Nature and mechanism of the metals ions adsorption from a ternary aqueous medium using natural sedimentary rock, Chem. Afr., 5 (2022) 1687–1702.
[21] F. Gomri, G. Finqueneisel, T. Zimny, S.A. Korili, A. Gil, M. Boutahala, Adsorption of Rhodamine 6G and humic acids on composite bentonite–alginate in single and binary systems, Appl. Water Sci., 8 (2018) 156, doi: 10.1007/s13201-018-0823-6.
[22] H.-J. Hong, H.S. Jeong, K.-M. Roh, I. Kang, Preparation of mesalazine-clay composite encapsulated alginate (MCA) bead for targeted drug delivery: effect of composite content and $CaCl_2$ concentration, Macromol. Res., 26 (2018) 1019–1025.
[23] N.M. Malima, S.J. Owonubi, E.H. Lugwisha, A.S. Mwakaboko, Thermodynamic, isothermal and kinetic studies of heavy metals adsorption by chemically modified Tanzanian Malangali kaolin clay, Int. J. Environ. Sci. Technol., 18 (2021) 3153–3168.
[24] A. Machrouhi, A. Elhalil, M. Farnane, F.Z. Mahjoubi, H. Tounsadi, M. Sadiq, M. Abdennouri, N. Barka, Adsorption behavior of methylene blue onto powdered *Ziziphus lotus* fruit peels and Avocado kernels seeds, J. Appl. Surf. Interfaces, 1 (2017), doi: 10.48442/IMIST.PRSM/JASI-V1I1-3.9022.
[25] R. Bassam, M. El Alouani, J. Maissara, E.H. El Khattabi, Y. Rachdi, N. Jarmouni, M.E.M. Chbihi, S. Belaaouad, Physico-chemical characterization of natural rocks and their valorization on the removal of arsenic from aqueous solution, Mater. Today Proc., 58 (2022) 1011–1019.
[26] M.E. Alouani, S. Alehyen, M.E. Achouri, M. Taibi, Comparative studies on removal of textile dye onto geopolymeric adsorbents, Environ. Asia, 12 (2019) 143153, doi: 10.14456/EA.2019.16.
[27] Y. He, L. Zhang, X. An, G. Wan, W. Zhu, Y. Luo, Enhanced fluoride removal from water by rare earth (La and Ce) modified alumina: adsorption isotherms, kinetics, thermodynamics and mechanism, Sci. Total Environ., 688 (2019) 184–198.
[28] Caracterisation de la kaolinite et du mica dans un kaolin enrichi, Sciences & technologie. A, sciences exactes, pp. 20–25.
[29] M. El Alouani, S. Alehyen, H. El Hadki, H. Saufi, A. Elhalil, O.K. Kabbaj, M. Taibi, Synergetic influence between adsorption and photodegradation of Rhodamine B using synthesized fly ash based inorganic polymer, Surf. Interfaces, 24 (2021) 101136, doi: 10.1016/j.surfin.2021.101136.
[30] H. Saufi, M.E. Alouani, J. Aride, M. Taibi, Rhodamine B biosorption from aqueous solution using *Eichhornia crassipes* powders: isotherm, kinetic and thermodynamic studies, Chem. Data Collect., 25 (2020) 100330, doi: 10.1016/j.cdc.2019.100330.
[31] S. Tunali Akar, F. Sayin, I. Ozdemir, D. Tunc, A natural montmorillonite-based magsorbent as an effective scavenger for cadmium contamination, Water Air Soil Pollut., 231 (2020) 409, doi: 10.1007/s11270-020-04743-3.
[32] A. Samad, M.I. Din, M. Ahmed, Studies on batch adsorptive removal of cadmium and nickel from synthetic wastewater using silty clay originated from Balochistan–Pakistan, Chin. J. Chem. Eng., 28 (2020) 1171–1176.